



## Molecular dynamics and Monte Carlo simulations of the sputtering of a nanoporous solid

J.F. Rodriguez-Nieva<sup>a,1</sup>, E.M. Bringa<sup>b,\*</sup>

<sup>a</sup> Instituto Balseiro, Universidad Nacional de Cuyo, 8400 Bariloche, Argentina

<sup>b</sup> CONICET & Instituto de Ciencias Básicas, Universidad Nacional de Cuyo, 5500 Mendoza, Argentina

### ARTICLE INFO

#### Article history:

Received 19 October 2012

Received in revised form 4 April 2013

Available online 15 April 2013

#### Keywords:

Sputtering

Atomistic simulations

Nanoporous material

Surfaces

### ABSTRACT

We calculate the sputtering induced on a nanoporous material by fast penetrating ions, such as those used for track formation and surface modification, in order to better understand and quantify the ejection and redeposition of atoms in open cell nanofoams. We model the ion-induced sputtering yield from a porous solid using a Monte Carlo approach and compare the results for the sputtering yields, angular and depth distributions of the ejecta, with Molecular dynamics simulations and find good agreement. For certain foam geometries, our simulations predict enhanced sputtering yields compared to the yields from a fully dense solid.

© 2013 Elsevier B.V. All rights reserved.

### 1. Introduction

Nanoporous materials appear under a number of conditions in basic and applied science: aerogels, activated carbon, metallic nanofoams, etc. Several fabrication methods allow features of characteristic lengths of 1–100 nm, making it possible to design materials with novel mechanical, thermal, electrical, optical and magnetic properties. Because of the high surface to volume ratio, full-density properties cannot be used for predictions. When we consider the interaction of radiation with nanoporous materials, the behavior can be very different from that of bulk materials, resulting in different surface evolution and restructuring.

Several applications can benefit from a better understanding of radiation damage at the nanoscale. Materials in fission and fusion reactors develop a porous structure due to radiation in the range eV–MeV, affecting the structural integrity, durability, mass and heat transport. For instance, fuel pellets from fission reactors develop a high-porosity structure due to the insolubility of the fission gases in the matrix [1]. Shielding materials in fusion reactors such as Tungsten can develop a nanoporous structure due to the large plasma fluences [2]. Surface modification of nanomaterials using ion beams can also benefit from such studies. Furthermore, materials in space (interstellar dusts, asteroids, comets) are generally porous. Ion irradiation is greatly responsible for surface weathering

and ejection of complex molecules into space, making porosity important for astro-chemistry [3].

There are no scaling laws for the sputtering yield as a function of porosity. The physical phenomena that take place is complex, and involve reduction of thermal conductivity due to the material confinement, angular and depth distribution of the ejecta being affected by the complicated geometry of the material, and re-deposition of atoms in the internal and external surfaces of the material. There are a number of continuum-level simulations related to the problem of predicting the evolution of surface roughness under ion bombardment [4,5]. This is related to the problem of irradiation of a porous material because it has to take into account bombardment of surfaces at different incident angles, re-deposition, etc. Monte Carlo (MC) simulations by Cassidy and Johnson [6] showed a large influence of porosity in the sputtering yield when the sticking coefficient of ejected atoms is large. In their study, bombarding ions deposit their energy within a distance from the surface much smaller than the mean pore radius. Therefore, in this case the decrease in yield is mostly associated with re-deposition of atoms ejected from internal surfaces of the sample. For bombarding energies below 0.5 keV, experimental and MC simulation results for the enhancement or decrease in the sputtering yield of compacted powder samples, as compared to full density samples, were very recently explained by the competition between enhanced angular sputtering and re-deposition effects from a rough target surface [7].

Current models and experiments could benefit from simulations at the atomic level. Molecular dynamic (MD) simulations follow the evolution of a system of atoms interacting through an

\* Corresponding author. Tel./fax: +54 261 423 6003.

E-mail address: [ebringa@yahoo.com](mailto:ebringa@yahoo.com) (E.M. Bringa).

<sup>1</sup> Present address: Massachusetts Institute of Technology, Cambridge, MA 02139, USA.

effective potential and have been used to study electronically induced sputtering [8]. Monte Carlo methods like SRIM [9] offer flexibility and speed in calculating sputtering yields, but cannot typically account for non-linear effects in the nuclear stopping regime, and would give zero sputtering yields in the electronic sputtering regime since a link between electronic energy deposition and lattice atomic motion is not provided. MD, on the other hand, is computationally costly but can reproduce experimental results for simple solids, like pure metals and semiconductors, and it can include chemical sputtering and electronic effects through different models [8]. Recently, plasma etching from a surface of SiOCH with nm-sized pores bombarded by 300 eV CF<sub>2</sub> ions was studied by Smirnov et al. [10], using MD. At normal incidence, sputtering yield for the porous sample (65% density) was 62.5% of the yield for the full density sample, but the behavior was complex regarding stoichiometry and at other incident angles.

We recently presented results on sputtering yield from a swift heavy ion thermal spike [3]. Here we use the results of the MD simulations for a thermal spike in a full density solid to parametrize a MC model of the sputtering yield of a porous solid. We then compare the MC results with an MD simulation of a nanoporous solid, and finally we discuss the range of validity and possible applications.

## 2. Simulation methods

The MD simulation for the nanoporous sample is described in detail elsewhere [3], and only a brief summary is provided here. We use a Lennard–Jones (LJ) potential to describe the interaction between simulated particles, which might represent atoms or whole molecules. The LJ potential has two parameters: a length  $\sigma$  and energy  $\epsilon$ . The number density  $r$  and cohesive energy  $U$  of the solid can be fitted using  $r = 1.055/\sigma^3$  and  $U \sim 8\epsilon$ , respectively. Simulations are dimensionless and, therefore, a given material can be chosen a posteriori to compare to laboratory data as needed [8,11,12]. The porous samples were generated as in Crowson et al. [13] A porosity of 45% was chosen for our simulations, with a distribution of ligament/grain sizes around 5–8 $\sigma$  (see Fig. 1(a)). This sample has  $\sim 195,000$  molecules. A thermal spike model [14,15] was used to describe lattice heating by the electronic excitations, with a heating time of 0.2 (expressed in Debye times), and a final temperature  $T \sim 1–30U$ , for a spike track of radius 1–10 $\sigma$ . 100 sputtering events were enough to give an error in the yield within a range of 3–10%.

For the MC simulations, instead of considering complex pore geometries, we describe the nanoporous material with a uniform

roughness model and two simple cases with cylindrical symmetry: pores with rectangular and sinusoidal cross-sections (Fig. 1(b)). The first geometry allows to study the atomic re-deposition effects which decrease the sputtering yield as in previous MC simulations [6,7]. The second geometry includes, additionally, the increase in the sputtering yield due to the increase of effective surface in the material. The relevant dimensionless parameters of the model are: the relative depth  $H/L$ , where  $H$  is the pore depth and  $L$  is the pore diameter; the relative inter-pore distance  $X/L$ , where  $X$  is the inter-pore distance and which is a measure of the grain/filament size ratio; and a scaling factor  $a_0/H$ , where  $a_0$  is the lattice parameter. Once an atom is ejected, it can escape the sample or collide with other atoms. In the latter case, the atom may stick or cause further sputtering. In our model we assume a sticking coefficient of 1 (i.e., all atoms stick). Radiation was assumed to be normally incident and uniformly distributed, and we set  $X/L = 1$ . Larger  $X$  would imply additional sputtering contributions from a flat surface, which is assumed to be known.

## 3. Results and discussion

MD simulations of a full density solid provided the necessary input for the MC simulations. Sputtering yield as a function of the incident angle  $\Theta$  are well described by  $Y(\Theta) \propto \cos^{-m}(\Theta)$ , with  $m = 1.6$ . This agrees extremely well with experiments for electronic sputtering of condensed gas solids [16] and insulators [17], as well as with previous MD simulations [18] and analytic models [19] where the energy was deposited instantaneously as a delta function in energy. We assume that sputtering goes to zero for incident angles larger than 80°, in agreement with experimental results [20] and simulation results [7], as plotted in Fig. 1(c). The angular distribution of the ejecta did not depend greatly on the angle of incidence of the ion, as also seen in experiments [17]. The distribution of the exit angle  $\theta$  of the ejecta with respect to the surface normal  $\mathbf{n}$  is well described by  $Y(\theta) \propto \cos^n(\theta)$ , with  $n = 3.0$ . This also agrees with experiments [17] and simulations [14]. However, we note that simulations at much lower energy density might lead to angular distributions approaching  $n = 1.0$ , and that much larger track radii might lead to even more forward peaking distributions.

Ejected particles in a full density sample originate extremely close to the surface, with a depth distribution  $\propto z^{-4}$ . As only a few layers of atoms  $\sim 4$  as in Bringa et al. [14] are important for sputtering, the scaling factor  $a_0/H$  will have little influence in the MC results and  $a_0/H$  was set to 0.

The energy distribution of ejected atoms is well described by a Sigmund–Thompson distribution [21], but could also combine a Maxwellian distribution and a Sigmund–Thompson distribution, as found in MD simulations [15] and used by Cassidy and Johnson [6] As the sticking coefficient was set to one, the energy of the ejected atom will have no effect on sputtering. Otherwise, large energies in the ejected atoms increase the probability of re-sputtering. The above distributions do not depend much on spike heating time, for times 0.01–2.

The angular and depth distributions of the ejecta are shown in Fig. 2. At normal incidence, the area being bombarded is always the same for the square pore, while for the sinusoidal pore the area increases as the value of  $H/L$  becomes larger. Because of the curvature effects, as we increase  $H/L$ , the dispersion of the distribution of the angle of ejection also increases for the sinusoidal pore, while the distribution becomes more peaked in the case of the square pore, as shown in Fig. 2(a). There is good agreement between the MD and MC simulations using  $H/L \sim 1$ , which is consistent with the geometry of the porous sample of Fig. 1(a). Additionally, there is always a significant contribution to the sputtering yield from the upper edge of the sinusoidal pore, as shown in Fig. 2(b). For values

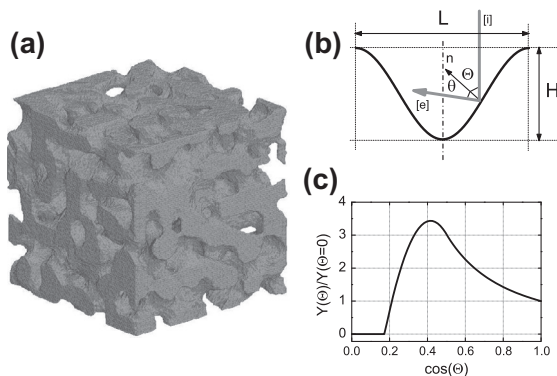


**Fig. 1.** (a) Initial sample of the MD simulation. (b) Sinusoidal pore geometry and relevant parameters and variables of the MC simulation. Here  $L$  and  $H$  are the diameter and depth of the pore, respectively,  $\mathbf{n}$  is the surface normal,  $\Theta$  is the angle between  $\mathbf{n}$  and the incident particle [i], and  $\theta$  is the angle between  $\mathbf{n}$  and the ejected particle [e]. (c) relative sputtering yield as a function of incident angle.

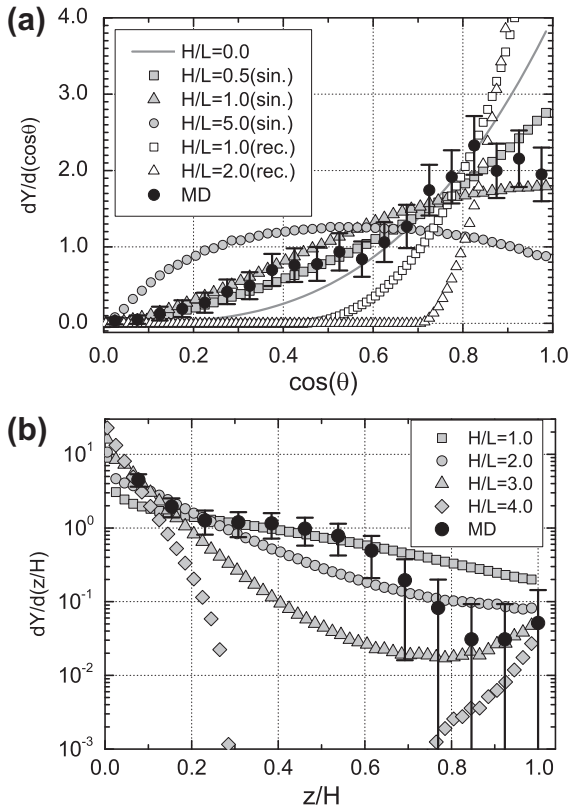


**Fig. 2.** Comparison of (a) angular distribution and (b) depth distribution of ejected particles obtained by MD and MC simulations. Shallow pores ( $H/L \rightarrow 0$ ) correspond to the distribution for surface ejection of a dense solid. Deep pores ( $H/L \rightarrow \infty$ ) correspond to depletion due to ‘jet-like’ ejection. The nanofoam sample of the MD simulations corresponds to  $H/L \approx 1-2$ . In the labels, sin. and rect. stand for sinusoidal and rectangular surface profiles.

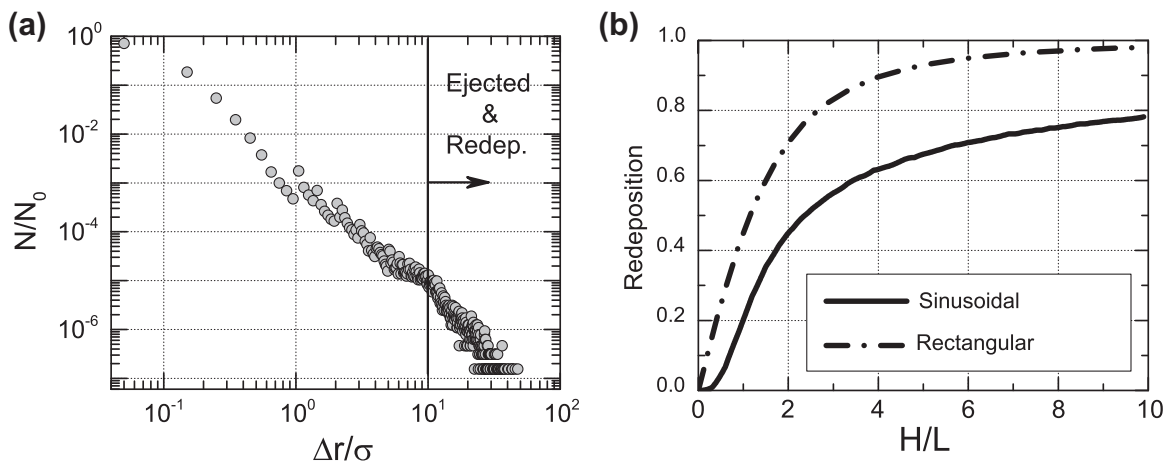
of  $H/L > 4$  we see that ejecta comes either from the edges of the pore or from deep inside the pore, where atoms are ejected with a forward distribution.

Visualization of our MD simulations for the nanoporous sample indicates that the ejected atoms either stick to opposite surfaces or escape if they were initially in a pore leading to a surface opening. In Fig. 3(a) we show the displacement distribution of atoms with respect to their original position in the MD simulations, and in

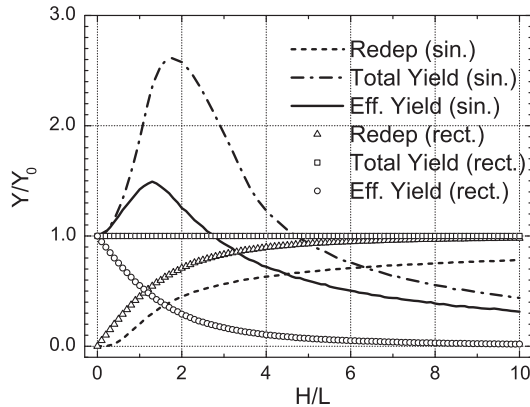
Fig. 3(b) we show the re-deposition according to our MC simulations. We can assume that an atom in the MD simulation that travels a distance  $\Delta r$  more than the size of a filament (i.e.,  $\Delta r > 5-10\sigma$ ) has been ejected and re-deposited in another surface (ejected atoms were excluded from the analysis of Fig. 3(a)). Clearly, ejected atoms which were initially located far from the surface (i.e., more than twice the size of the filament from the surface) would re-deposit. However, if we consider a surface layer of thickness  $15\sigma$  (i.e., twice the average filament size) and consider only atoms which are ejected ( $\Delta r > 10\sigma$ ), we obtain that approximately 40% of the atoms are re-deposited, while the rest are ejected without collisions. This is consistent with the MC results of Fig. 3(b) at  $H/L \sim 1$ . We also see from Fig. 3(b) that, for the rectangular pore, redeposition rapidly converges to  $\sim 1$ , but for the sine pore it goes slowly to a roughly constant value  $\sim 0.8$ . This is because the top part of the pore behaves nearly as a flat surface and always contributes to the sputtering.

Fig. 4 shows the results for the total and effective sputtering yield  $Y$  and  $Y_{\text{eff}}$ , where the total sputtering yield does not take into account redeposition while the effective sputtering yield does. For the sinusoidal pore, the effective sputtering yield remains close to 1 for  $H/L < 4$  and then decreases slowly because of the competition between redeposition and the sputtering enhancement due to the curvature effects. Instead, for the square pore there is a rapid decrease due to the large re-deposition seen in Fig. 3(b) and no enhancement due to curvature effects. Using MD simulations, we find that the sputtering yield for the described nanoporous solid is the same as that of the full-density solid [3]. This effect is reproduced in the MC calculations of the present paper, as shown in Fig. 4. This is contrary to several studies and models [6,22,23], which show a reduction in the sputtering of a porous solid when compared to the sputtering of the non-porous solid. If we consider the case of porous solids where the bombarding ions can penetrate deeply into the material ( $H/L > 5$ ), then we would have a case similar to the one described by Cassidy and Johnson [6], and sputtering yield values would indeed decrease compared to bulk values. However, if bombarding ions do not penetrate deeply into the material, the sputtering yield will not be necessarily reduced because of the competition between surface curvature enhancement and redeposition effects.

Our approach can be easily generalized to include more general situations, such as off-normal incidence and re-sputtering. For sputtering induced by electronic excitations, the energy of the ejecta is very low and would not lead to re-sputtering. On the other



**Fig. 3.** (a) Distribution of displacements in the MD simulation. Here  $\Delta r$  represents the net displacement of atoms between the initial and final configurations of the simulation. (b) Fraction of atoms that are redeposited in the opposite surface as a function of the depth of the pore by MC. Reasonably good agreement is obtained between the MD simulation (redeposition of  $\sim 40\%$ ) and the MC simulation (redeposition in the range 20–45%).



**Fig. 4.** Total and effective sputtering yields normalized by the flat surface sputtering yield  $Y_0$ , and redeposition factor  $R$ . The effective sputtering yield is calculated as  $Y_{\text{eff}} = Y_{\text{tot}}(1 - R)$ , where  $Y_{\text{eff}}$  is the (normalized) effective yield, and  $Y_{\text{tot}}$  is the total yield. In the labels, sin. and rect. stand for sinusoidal and rectangular surface profiles.

hand, nuclear sputtering by keV projectiles might produce ejecta with enough energy to re-sputter. Additionally, sticking coefficients different from 1 for sputtered particles might apply for some molecular species with very low reactivity. Finally, inclusion of the separation between pores, i.e. the grain/filament size as another variable, may affect the sputtering yield. The size effect can become important when the grain size divided by the ion range becomes smaller than approximately 3 [24]. However, there are other effects which cannot be factored easily into the code: if the filament/grain size is small, thermal effects due to the confinement of the material might lead to changes in the ‘local’ sputtering yields when compared to the case of a fully dense solid. In addition, the code assumes that impacts are independent, which is valid for the experimental fluences used to study sputtering yield, but invalid at the large fluences used for surface patterning.

#### 4. Conclusions

We modeled the sputtering from a one component nanoporous solid. Our Monte Carlo approach can be used for a large number of situations, since the input consisting of energy, angular and depth distributions can be obtained from both experiments and simulations for fully dense solids. For instance, there is a large body of results for sputtering induced by keV ions, which could be used as input, taking into account the limitations of our approach.

Sputtering yield at the nanoscale is dominated by ejection of atoms from the enhanced surface area near the top surface. If we consider voids in the micron range, then the scenario is described as in Cassidy and Johnson [6]. This differs from the density-depleted sample we have simulated atomistically, where width and extent of a single ion track overlaps several grains, and where pores and grains are much smaller than the penetration depth of the ion. Using MD simulations we found in previous work [3] that the sputtering is about the same for the porous and bulk samples when characteristic pore sizes are up to a few times larger than grain/filaments sizes. Here we obtain similar results using Monte Carlo simulations, in which we show that sputtering can even be enhanced due to the increased effective surface for values of  $H/L < 3$ , where  $H$  and  $L$  represent the characteristic depth and width of the pores, respectively.

Our Monte Carlo simulations combined with MD simulations open the possibility for parametric studies which can help guiding experiments on radiation modification of nanoporous solids under a variety of conditions, from nuclear reactors to astrophysics. A way to confirm our results is to measure sputtering from metallic foams for heavy keV projectiles, where electronic sputtering might

be negligible, or sputtering from swift heavy ions bombarding sub-micron/micron powders, like silica and alumina powders which are readily available.

#### Acknowledgements

We thank R. Baragiola for insightful discussions, and Diana Farkas for providing the foam sample. E.M.B. thanks support from the CONICET and PICT2009-0092, and J.F.R.N. thanks support from a scholarship from the Comisión Nacional de Energía Atómica (CNEA).

#### References

- [1] K. Nogita, K. Une, Radiation-induced microstructural change in high burnup  $\text{UO}_2$  fuel pellets, *Nuclear Instruments and Methods in Physics Research Section B: Beam Interactions with Materials and Atoms* 91 (1994) 301–306.
- [2] S. Takamura, N. Ohno, D. Nishijima, S. Kajita, Formation of nanostructured tungsten with arborescent shape due to helium plasma irradiation, *Plasma and Fusion Research* 1 (2006) 051–051.
- [3] J.F. Rodríguez-Nieva, E.M. Bringa, T.A. Cassidy, R.E. Johnson, A. Caro, M. Fama, M.J. Loeffler, R.A. Baragiola, D. Farkas, Sputtering from a porous material by penetrating ions, *The Astrophysical Journal Letters* 743 (2011) L5.
- [4] M.A. Makeev, A.L. Barabási, Effect of surface morphology on the sputtering yields. II. Ion sputtering from rippled surfaces, *Nuclear Instruments and Methods in Physics Research Section B: Beam Interactions with Materials and Atoms* 222 (2004) 335–354.
- [5] J. Muñoz-García, R. Gago, L. Vázquez, J.A. Sánchez-García, R. Cuerno, Observation and modeling of interrupted pattern coarsening: surface nanostructuring by ion erosion, *Physical Review Letters* 104 (2010) 026101.
- [6] T. Cassidy, R. Johnson, Monte Carlo model of sputtering and other ejection processes within a regolith, *Icarus* 176 (2005) 499–507.
- [7] F. Boydens, W. Leroy, R. Persoons, D. Depla, The influence of target surface morphology on the deposition flux during direct-current magnetron sputtering, *Thin Solid Films* 531 (2013) 32–41.
- [8] E.M. Bringa, R.E. Johnson, Coulomb explosion and thermal spikes, *Physical Review Letters* 88 (2002) 165501.
- [9] J.F. Ziegler, J.P. Biersack, M.D. Ziegler, SRIM. The Stopping and Range of Ions in Matter, Lulu Press Co., Morrisville, NC, USA, 2012.
- [10] V.V. Smirnov, A.V. Stengach, K.G. Gaynullin, V.A. Pavlovsky, S. Rauf, P.L.G. Ventzek, A molecular dynamics model for the interaction of energetic ions with sioch low- $\kappa$  dielectric, *Journal of Applied Physics* 101 (2007).
- [11] E.M. Bringa, R.E. Johnson, A new model for cosmic-ray ion erosion of volatiles from grains in the interstellar medium, *The Astrophysical Journal* 603 (2004) 159.
- [12] E.M. Bringa, S.O. Kucheyev, M.J. Loeffler, R.A. Baragiola, A.G.G.M. Tielens, Z.R. Dai, G. Graham, S. Bajt, J.P. Bradley, C.A. Dukes, T.E. Felter, D.F. Torres, W. van Breugel, Energetic processing of interstellar silicate grains by cosmic rays, *The Astrophysical Journal* 662 (2007) 372.
- [13] D.A. Crowson, D. Farkas, S.G. Corcoran, Mechanical stability of nanoporous metals with small ligament sizes, *Scripta Materialia* 61 (2009) 497–499.
- [14] E. Bringa, R. Johnson, L. Dutkiewicz, Molecular dynamics study of non-equilibrium energy transport from a cylindrical track. Part II. Spike models for sputtering yield, *Nuclear Instruments and Methods in Physics Research Section B: Beam Interactions with Materials and Atoms* 152 (1999) 267–290.
- [15] E.M. Bringa, R.E. Johnson, M. Jakas, Molecular-dynamics simulations of electronic sputtering, *Physical Review B* 60 (1999) 15107–15116.
- [16] W. Brown, W. Augustyniak, K. Marcantonio, E. Simmons, J. Boring, R. Johnson, C. Reimann, Electronic sputtering of low temperature molecular solids, *Nuclear Instruments and Methods in Physics Research Section B: Beam Interactions with Materials and Atoms* 1 (1984) 307–314.
- [17] M. Toulemonde, W. Assmann, C. Trautmann, F. Grüner, Jetlike component in sputtering of LiF induced by swift heavy ions, *Physical Review Letters* 88 (2002) 057602.
- [18] E. Bringa, R. Johnson, Angular dependence of the sputtering yield from a cylindrical track, *Nuclear Instruments and Methods in Physics Research Section B: Beam Interactions with Materials and Atoms* 180 (2001) 99–104.
- [19] R.E. Johnson, B.U.R. Sundqvist, A. Hedin, D. Fenyő, Sputtering by fast ions based on a sum of impulses, *Physical Review B* 40 (1989) 49–53.
- [20] A. Oliva-Florío, R.A. Baragiola, M.M. Jakas, E.V. Alonso, J. Ferrón, Noble-gas ion sputtering yield of gold and copper: dependence on the energy and angle of incidence of the projectiles, *Physical Review B* 35 (1987) 2198–2204.
- [21] P. Sigmund, Theory of sputtering. I. Sputtering yield of amorphous and polycrystalline targets, *Physical Review* 184 (1969) 383–416.
- [22] B. Hapke, On the sputter alteration of regoliths of outer solar system bodies, *Icarus* 66 (1986) 270–279.
- [23] M.J. Loeffler, C.A. Dukes, R.A. Baragiola, Irradiation of olivine by 4 keV  $\text{He}^+$ : simulation of space weathering by the solar wind, *Journal of Geophysical Research (Planets)* 114 (2009) 3003.
- [24] S. Jurac, R.E. Johnson, B. Donn, Monte carlo calculations of the sputtering of grains: enhanced sputtering of small grains, *The Astrophysical Journal* 503 (1998) 247.